Discover Materials

Research

Green perspective of N-CDs towards energy crisis and photodegradation of toxic dyes

Mohd Abdullah Sheikh[1] · R. S. Chandok[2] · Khan Abida[3]

Received: 4 December 2023 / Accepted: 22 March 2024
Published online: 31 March 2024
© The Author(s) 2024 OPEN

Abstract
Here we have presented a general overview of an environmental friendly, one-step, cost-effective, and efficient microwave irradiation method for the preparation of self heteroatom doped Nitrogen doped carbon dots (N-CDs) which demonstrated an average size of less than 10 nm and an interplaner distance of 0.334 nm. These N-CDs possess 2.35 eV energy gap with 65.5% fluorescence quantum yield. The surfaces of these graphitic-like structures are doped with (S, P, K, Mg, Zn) = 1% along with the extra passivating agent nitrogen (N). They have demonstrated wider absorption (between 300 and 550 nm) and emission (between 400 and 600 nm) bands and also managed enormous active surface sites and defects, that further extend its usage in energy harvesting, storage and photo catalysis owing to their unique property of electron transport and collection system. In addition, we have prepared, tested, and optimised new TiO_2/N-CDs composite as photo anode and N-CDs/CB composite as photo cathode for application in dye-sensitized solar cells (DSSC). The achieved power conversion efficiency of the DSSC employed photoanode N-CDs/TiO_2 and counter electrode carbon black/N-CDs, demonstrated a substantial improvement, in photo current and photo voltage owing to their multiple factor visible light absorption, effective electron separation, and longer recombination time resulted a Jsc. of 22.90 mA cm^2, Voc. of 0.780 V, FF. of 74% and an overall PCE of about 13.22% approximating 2.5-fold increase in power conversion efficiency as compared to that of pure TiO_2 and platinum based DSSC, where Jsc. (= 10 mA cm^2), Voc. (= 0.750 V) and a total of 5.42% power efficiency. Furthermore, TiO_2 was modified with Heteroatom-doped N-CDs using a novel ultrasonic immersion technique, and demonstrated greater photocatalytic activity for the degradation of methylene blue (85%) with a rate constant of 0.1068 in accordance with the pure TiO_2 film and N-CDs which have showed only 20% and 30% photodegradation with lower rate constants under short UV irradiation, demonstrating the formation of reactive oxygen species and H^+ ions in the sample solution resulting enhanced effective mobility of electrons and holes between TiO_2/N-CDs composite nanomaterial, resulted greater photo degradation.

Keywords Heteroatom doped N-CDs · Microwave-irradiation · N-CDs · TiO_2 based DSSC · Degradation of MB · Nitrogen passivation agent

✉ Mohd Abdullah Sheikh, absheikh1989@gmail.com; R. S. Chandok, rschandok_68@yahoo.com; Khan Abida, khanabidamajid8179@gmail.com | [1]Bhagwant University, Ajmer, India. [2]Sri Guru Tegh Bahadur Khalsa College, Jabalpur, India. [3]Shaheed Himayun Muzzamil Memorial, Government Degree College, Anantnag, J&K, India.

1 Introduction

Carbon dots (CDs) are made by pyrolyzing materials with high carbon content. As a consequence of the significant changes in their physical and chemical characteristics, CDs have a regulated emission wavelength and a high quantum yield. The structure is chaotic due to the differing amounts of carbon to carbon rich conjugated type sp^2 in the inner core, dispersed in a gem type sp^3 conjugated carbon framework [1–4]. Typically, the lattice spacing is 0.34 nm, and its semi-spherical shape has a diameter of up to 10 nm and vertical dimensions of less than 5 nm [5, 6]. Apart from the central core, the CD framework consists of two separate sections: the surface state and the molecular state, hydroxylic, carbonic, carboxylic, amino, and sulphide groups are the main heteroatomic binding sites that produce the surface state of CDs. The molecular state's individual chromophores function analogous to organic colours. CDs have better photochemical characteristics and stronger intrinsic photoluminescence when compared to other nanocarbon [7, 8]. The production of multicoloured light-emitting diodes (LEDs), efficient energy transmitters and live storage, in-vivo studies, photocatalytic degradation, drug delivery, and fluorescent sensors are just a few of the novel areas of application that have been discovered as a result of these materials' excellent compatibility, efficient stability towards light, low cytotoxicity, simple surface modification, and inert chemical behaviour [9–29]. There are two distinct kinds of carbonaceous raw materials that can potentially be employed for the creation of C-Dots [30]: biological and chemical carbon sources. On the context of sustainability, biomass precursors [31–34] have the potential to be utilised for the creation of carbon dots owing to their reasonable amount, universal availability, environmental friendliness, as well as their ability to organizing biological waste. Moreover, they provide a large number of spontaneous ingredients, including lignin, cellulose, lignocellulose, carbohydrates, proteins, triglycerides, and naturally occurring elements like iron, phosphorus, zinc, magnesium, and manganese, which serves as powerful self-dopants, for the multipurpose activities and also raised the quantum yield efficiency.

Researchers have been able to improve the electro-catalytic performances of carbonaceous materials by doping heteroatoms such as (N, B, P, S, and so on) into the carbon nano-structure. For example nitrogen-doping into carbon nanomaterials including CNTs, graphene, and GCDS have been researched and have found many advantages over non doped carbon nano materials [35]. In the fields of energy storage, dye photodegradation, and light harvesting, these beneficial qualities are of great interest.

Dye sensitized solar cells (DSSCs) have received a lot of interest as a viable alternative to conventional silicon-based photovoltaic cells [36] owing to their affordable production costs, excellent conversion rate, ecological compatibility, as well as simple fabrication procedures [37–40]. However, transition-metal oxides (TMOs) such as TiO_2 [41], ZnO [42], WO_3 [43], and RuO_2 [44] have attracted substantial attention owing to their unique layered structure and diverse electronic and optical characteristics, amongst these materials, titanium dioxide (TiO_2), exhibited the greatest light absorption behaviour, has drawn significant interest and has been widely used in photovoltaic's, photo electrochemical cells, photocatalysis, and gas sensing [45–49]. However, because of its smaller surface area, wider bandgap, and rapid electron–hole pair recombination, leads to the overall PCE of just (5–10)%. Therefore, In-situ combinations of TiO_2 with nano carbonous materials along with nitrogen and other trace element doping are promising alternatives to address these problems, owing to their viability, direct accessibility, enormous surface area, efficacy in electrochemical environments, creation of adequate active sites, tuning of the TiO_2 bandgap, and widening of the charge recombination process has improved the overall photocatalytic properties [50]. However, the use of N-CQDs as a co-active layer in addition to TiO_2 also makes it easier to modify the photo-anode's band structure and can reduce recombination between the electrolyte and the photo-anode [51] and also demonstrated improved effectiveness when utilised as co-sensitizers with ion selective quantum dots (ISQDs) [52] or organic dyes [53] because, by utilising the carbon dots as co-sensitizers, spare exploitable light can be used to broaden the absorption zone and enhance the charge extraction process in perovskite solar cells [54–56]. While in, CD/TiO_2 based DSSCs efficiently harvest the solar spectrum, transferring UV region to the visible region, and shield the photosensitizer from deterioration and provide more stability [57, 58].

In the whole photoelectric conversion process, the counter electrodes (CEs) of the DSSC play a key role for capturing of electrons and lowering of the overall potential for the reduction of I^{3-} to I^- in the redox electrolyte [59, 60]. They are typically constructed from vacuum-deposited platinum (Pt), which is placed on a conducting glass (FTO), as Pt is one of the most expensive materials, although having good electrical conductivity, stability, and catalytic activity, its non-renewability prevents DSSC's from becoming widely used. As a result, the primary requirement for a material to replace Pt as a catalyst in a DSSC includes a lower charge-transfer resistance and a high exchange current

density for the reduction of the oxidised form of the charge mediator. The nano-sized carbonous material has shown a charge-transfer resistance of 0.74 cm^2 [61–64], which is approximately two times lower than the charge-transfer resistance of a screen-printed Pt CE and achieved a photo-conversion performance of 7.56% and these substances have showed chemical and electrochemical stability in the cell's electrolyte system. In light of these issues, carbonaceous materials have been widely used as Pt substitute catalysts to minimise the expenditures while maintaining the DSSC's performance [65], for instance GQDs were decorated with PPy on fluorinated tin oxide (FTO) glass as a very effective but low-cost CE for high-performance DSSCs [66, 67] solely due to their greater inherent catalytic activity. In another investigation, $CoSe/GN_{0.50}$ CE outperformed pure CoSe and platinum in terms of photovoltaic performance [68]. Several groups have also investigated carbon black as a CE for DSSCs [69, 70], which has also demonstrated remarkable long-term electrochemical stability in I^{3-}/I^- electrolyte [71, 72].

Rapid economic and industrial growth in recent years has led to an increase in the amount of hazardous wastewater into water resources, including groundwater, surface water, and drinking water supplies. Unfortunately, many contaminants are generally long-lasting and can degrade only in harsh environments (high temperature, high alkalinity, ultraviolet (UV)) as well as under certain chemical and physical processes. When wastewater is treated severely, hazardous chemicals are utilised or the byproducts are created which usually are more damaging to the surrounding ecosystem than the original component. Therefore, to eliminate toxins from the environment, current wastewater treatment techniques must be replaced with more effective ones [73]. In order to safely clean wastewater, photocatalytic degradation is a method that is frequently used [74–76], using semiconductors as catalysts under irradiation, have been proposed as an environmentally friendly method for treating organic pollutants [77] which employs advanced oxidation processes (AOPs), relied on the production of reactive oxygen species (ROS), such as hydroxyl radicals $OH^{\bullet}$ and singlet oxygen species. The most widely used catalyst for photocatalytic degradation is TiO_2 nanoparticles, because of low toxicity, chemical inertness, high catalytic effectiveness, and cheap cost [78]. However, TiO_2 has certain drawbacks, including quick electron–hole recombination, broad short UV band gap energy, high concentration aggregation, and an insufficient specific surface area, which bounds the effectiveness of its efficiency of photodegradation. As a result, the modification of carbonaceous substances on the surface of TiO_2 has been recommended as a remedy for these problems, so that, the photoexcited electrons in TiO_2 may be transported to carbonaceous substances, which might serve as the binding centres for electron–hole pairs and prevent electron and hole recombination, hence increasing the photocatalytic efficiency of TiO_2 [79–82]. Numerous investigations have concentrated on creating CQD/TiO_2 nanocomposite materials with improved photocatalytic activity for the destruction of organic pollutants, for instance Rhodamine B and cefradine were subjected to UV irradiation by Chen et al. [83] to determine the photocatalytic activity of carbon quantum dots/TiO_2. Furthermore, doping light heteroatoms (B, N, P, and S) into CQDs can significantly boost the electrical conductivity and specific surface area [84, 85] hence increased photocatalytic performance. Therefore, it is anticipated that heteroatom-doped CDs will improve the TiO_2's photo-catalytic capacity for the removal of hazardous chemicals.

This section provides a comprehensive summary of the most recent review papers, focusing on the developments in the overall study and creation of hetero-atom-doped CDs with an appropriate citing [86–88]. These review papers have mainly concentrated on the various synthetic strategies, for the preparation of hetero-atom-doped CDs due to their distinct qualities and potential in a range of applications, They have looked at a number of synthetic strategies, ranging from different raw materials to different synthetic methods and incorporated different doping elements in order to further improve the overall optical, biological, and catalytic properties of hetero-atom-doped CDs and their wide range of applications in nano-probes, optoelectronic devices, catalysis, and biomedicine. Hetero-atom doping is an efficient way to improve the optical, electrical and chemical characteristics of CDs by inserting atomic impurities (nitrogen, boron, sulfur, phosphorus, etc.) into the CD's surface, altered its electronic structure producing n-type or p type CDs hybrid material.

However, we have prepared the N-CDs from biomass derived pumpkin seeds for the first time by microwave irradiation method through green approach and added urea as nitrogen source to achieve the required doping of nitrogen element besides the nitrogen certain elements like sulpher, phosphorus and zinc which are the characteristics of pumpkin seed composition have also been added in the percentage of less than 1 (< 1%) to modify the surface functional groups, surface dislocation and provides enormous active sites for the various application purposes and provided an overall P type character of these prepared N-CDs with their av. size of 8–10 nm. They have shown an enormously good quantum yield (QY) of 65.5% against the previously prepared low quantum yielded N-CD's, besides that they provided excellent optical properties both in absorption and excitation dependent photoluminescence (PL) properties with an energy band gap of only 2.35 eV against the previously synthesized high bandgap N-CDs. These prepared N-CDs have demonstrated excellent electrochemical activity in both oxidation and reduction perspectives, provided high energy density storage hence can be used in supercapacitors, besides that they have demonstrated antifungal activity and bio imaging of "Cladosporium

cladosporioides" responsible for economic loss in food industry [89]. Here, in this work these novel self heteroatom doped N-CDs (5%) were mixed with carbon black and employed as a modified innovative semi-transparent counter electrode annealed at 450 °C assembled with the generated heteroatom nitrogen doped carbon nano dots optimized Weight% of (30%) with TiO_2 as a co-active material or novel photoanode for developing a novel DSSC cell, N719 dye as a sensitizer and I^{3-}/I^- as electrolyte. Upon illumination, the photo-generated electrons transferred to the N-CDs and TiO_2 co-active material composite and accumulated holes in the N719 dye's valence band, hence effectively separated the charge carriers and extended the lifetime of the electrons. Most notably, adding these hetero-atom doped NCQDs to TiO_2 makes it easier to modify the photo-anode's band structure and therefore, reduces interaction between the I_3^-/I^- electrolyte with the photo-anode resulting in a Jsc of 22.90 mA, Voc of 0.78 V, and FF of 0.74, providing a total PCE of 13.22% cm^{-2}.

In addition, a composite made of N-CQDs and TiO_2 exhibited high photocatalytic activity towards degradation of azo dyes like Methylene blue under short UV light has been demonstrated in this study. For this purpose, an ultrasonic dispersion method was used to decorate the TiO_2 particles by these hetero-atom doped N-CQDs, after that under UV light leading to formation of ROS in solvent system, owing to their multiple active sites and defects, resulting in the adsorption and reduction of oxygen on the surface, which prevents the recombination of electrons and holes in the TiO_2 and enhanced the photocatalytic efficiency of N-CDs/TiO_2 hybrid material from 30 to 85% against degradation of MB in 18 min of short UV irradiation period, while as pure TiO_2 film and pure N-CDs as a solo photocatalysts demonstrated only 20% and 30% of degradation towards MB dye.

2 Experimental sections

2.1 Preparation

Our group Abdullah et al. [89] recently published a novel work, detailing the sample preparation as well as all other characterizations with application. This introduction provides a brief explanation of their features and preparation. Starting precursor, pumpkin seeds were used as a carbon source to create self heteroatom doped N-carbon dots and the process of surface passivation, also known as surface state change, is carried out by supplying nitrogen from "urea". After being exposed to microwave pyrolysis, through centrifugation and filtering a light brown fluid was produced. The amount of urea fixing was set at 3 g, and the amounts of pumpkin seeds, microwave power, and reaction time were all gradually changed to get a high fluorescence quantum yield. The QY first increased as the quantity of pumpkin seeds in these CDs increased and then peaked at 3 g. After that, the limit of pumpkin seeds at 3 g with a quantum yield of 65.5% was optimised using a microwave irradiation power of 900 W and 8-min reaction duration. To produce CDs with a high QY, the precursor needs to be properly carbonised, and this can only be done at a temperature and reaction time that are both enough. However, a much higher reaction temperature and a longer reaction time might eliminate the emissive sites, which would reduce QY.

3 Results and discussion

3.1 Characterization and properties of self-hetero atom doped N-carbon dots

Pumpkin seeds shown in Fig. 1a were used for the first time as a carbon source to create self heteroatom doped N-carbon dots, along with "urea" as a nitrogen source for surface passivation or surface modification proceeded with the microwave irradiation reaction for certain minutes, a light brown solid paste was produced followed by filtration, centrifugation and dialysis, a yellow solution was produced as exposed to sunlight, and showed a fluoresced cyan color illuminated under UV light as illustrated in Fig. 1b and c, respectively. Achieving a high fluorescence quantum yield required incremental optimization of the amount of urea (set at 3 g), the number of pumpkin seeds, microwave power, and reaction time. As the pumpkin seed content grew, the quantum yield QY of these CDs initially increased and then decreased until it peaked at 3 g. Then, using a microwave irradiation power of 900 W and an 8-min reaction period, the number of pumpkin seeds at 3 g with a quantum yield of 65.5% was optimized. To create CDs with a high (QY), the precursor must only be suitably carbonized for a suitable amount of time and at a sufficient temperature. However, the QY, has decreased due to eradication of the generated emissive sites by a significantly higher reaction temperature and longer reaction time [89].

Fig. 1 **a** Pumpkin seed precursor **b** Carbon dots under visible light **c** carbon dots under UV light

The morphology, size distribution, elemental analysis and optical properties of as prepared N-CDs was previously published by our group Abdullah et al. [89] through Springer publishing company and the results have demonstrated that the N-CDs have uniform size distribution with 5–8 nm average size, besides that the X-ray diffraction pattern clearly showed wide peak at 20°–40° which also denoted the production of tiny nanoparticles. The major peak at 24° revealed graphitic like core structure and an interplaner distance of 0.334 nm and confirmed the (002) lattice planning. Furthermore, the FTIR spectroscopy demonstrated the various surface functional entities such as O–H, N–H, COO–/amide II, C=C/C=N/C=O and C–H that makes the surface active with oxygen reactive species of these N-CDs, and were very effective for application point of view. The EDX analysis suggested that the following weight percentages were present: 48.3% C, 32.6% O, 18% N, 0.2% Mg, 0.2% P, 0.2% S, 0.3% K, and 0.2% Zn mainly because of complex nutritional value of pumpkin seeds.

A wide absorption zone covering a wavelength range of 254–550 nm was established by the optical characteristics. The main peak at 327 nm is due to the n–π* transition of C=N, C=O in the N-doped CDs, while the other tiny absorption peaks at 254 and 278 nm are generated by the π–π* transaction of the C=C interaction. Their excitation wavelength spanned from 380 to 480 nm, while the emission wavelength was red-shifted from 462 to 542 nm. Additionally, the optimal emission and excitation wavelengths for the N-doped CD solution were 462 nm and 380 nm, respectively. The N-doped CD's aqueous solution showed blue, cyan, green, and yellow hues at different stimulated wavelengths. When stimulated at longer wavelengths, the spectra redshifted and showed a typical excitation wavelength dependency. The behavior of N-doped CDs has been attributed to different diameters or different emissive spots on their surfaces. Consequently, it has been suggested that these N-doped CDs have sensing capabilities. Previous articles have also reported the excitation-dependent emission characteristic of carbon dots, further under constant irradiation at 380 nm for 5 h; since, the fluorescence intensity was unchanged without photobleaching, indicating their relatively strong photostability.

Based on the absorption spectroscopy results, the Tauc plot approach was used to determine and confirm the direct bandgap energy of these synthesized N-CDs, which is around 2.35 eV (or 527 nm). The reference standard quinine sulphate, dispersed in 0.1 mol of H_2SO_4 was used for the determination of the total quantum efficiency of the generated N-CDs and was calculated to be almost 65.50 percent, our group Abdullah et al., has previously published the same [89].

3.2 *Structural and morphological properties of TiO_2/N-CDs and CB/N-CDs composite*

The detailed SEM and EDAX of N-CDs are illustrated in our previous work Abdullah et al. [89] as they demonstrated a size range of 5–8 nm, an interplaner distance of 0.34 nm and the doping concentration of 48.3% C, 32.6% O, 18% N, 0.2% Mg, 0.2% P, 0.2% S, 0.3% K, and 0.2% Zn incorporated into the anatase pristine tetragonal structure of TiO_2 material. Here we have a proceeded with a full FTIR spectroscopy (500–3500 cm^{-1}) to indentify the surface functional groups and edge states. The FTIR spectroscopy is shown in Fig. 2 and has demonstrated the incorporation of N-CDs into the edge sites of anatase TiO_2 Let us begin with the composition of N-CDs as the broad peak at 3360 cm^{-1} is related to the O–H and N–H stretching while as a small peak at 2950 cm^{-1} is related to CH_2 stretching, while as the peaks at 1642, 1537 and 1393 cm^{-1} are related to the C=O stretching in amides, N–H deformation in amides and OH bending in carboxylic groups and the

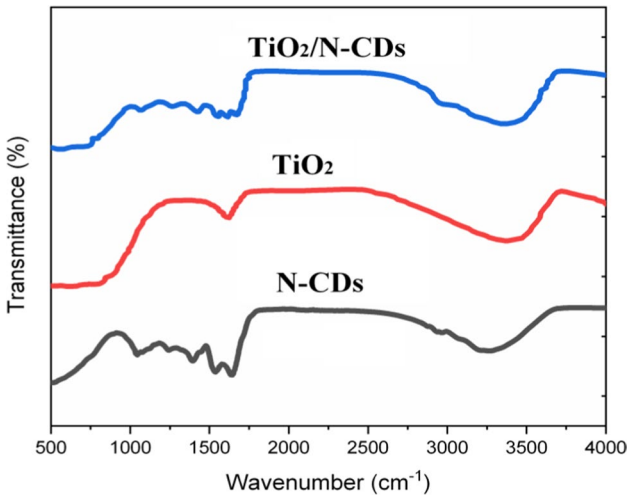

Fig. 2 FTIR spectra of N-CDs, TiO_2 and TiO_2/N-CDs composite showing strong linking of N-CDs onto the surface of TiO_2

small peaks at 1240, 1043 are associated with C-N and starching of C–O bonds, respectively. In addition to that, the small bands under 500 cm^{-1} showed a fever self heteroatom-doping elemental composition. The FTIR of TiO_2 tells us that the broad peak at 3300 $cm^{-1}$and another at 1628 cm^{-1} are related to O–H stretching and bending vibrations and a broad band under 1000 cm^{-1} belongs to the pure characteristic peak of TiO_2. However, TiO_2/N-CDs composite demonstrated all the peaks of N-CDs and a broad peak extended from 500 to 1000 cm^{-1} is associated with Ti–O–Ti/Ti–O–C vibrations, while as the narrow band at 2930 cm^{1} associated with C-H and represents the surface stabilization of carbon dots onto the TiO_2 sample.

Further we have checked the crystal structural morphology of TiO_2/N-CDs composite by X-Ray Diffractometer at 0.154 nm wavelength using Cu K(β) radiation and the variation in the structure of TiO_2 after doping with N-CDs is shown in Fig. 3. The results showed slight decrement in peaks positioned at 25.3° and 37.8° which are related to (101) and (004) planes of anatase phase clearly demonstrated the prevention of agglomeration of TiO_2 particles, otherwise there is no significant effect of these N-CDs on the crystal structure of TiO_2. Further the slight increment in the peaks positioned at 48.3°, 54.1°, 55.1° and 62.8° are related to the (200), (105), (211) and (204) planes which demonstrated that the N-CDs are attached at the edge surfaces towards lateral sides. In order to fully understand the structure of TiO_2/N-CDs nanocomposite, the crystal structure is demonstrated in Fig. 4, where the N-CDs are attached to the surface of tetragonal structure of pure anatase phase of TiO_2 material filling the mesoporous cavities in the TiO_2 structure.

However, in case of counter electrode the N-CDs as well as the CB is amorphous in nature therefore upon mixing them there is no significant variation in the nature of structural morphology, however the surface functional groups of N-CDs are added to the CB/N-CDs composite making them photoactive and more productive as charge carrier receiver and mediator catalyst for effective reduction of I^-/I_3^- while as, the PVDF binder provides a good adhesion between nanoparticles, carbon black and FTO glass to reduce the charge transfer resistance as well as the internal resistance which in turn provides long term stability of CB/N-CDs composite counter electrode. According to the previous studies the N-CDs are

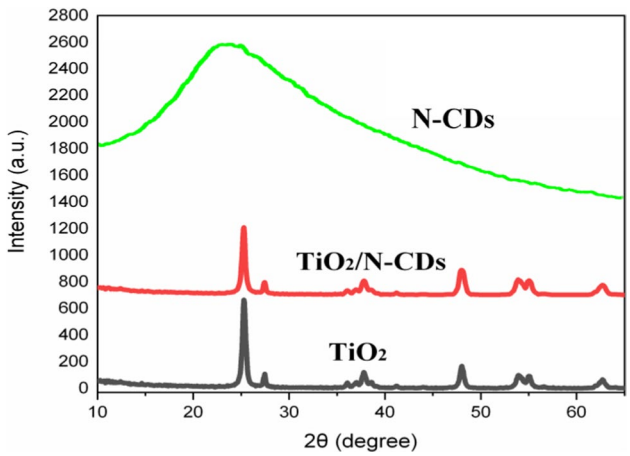

Fig. 3 XRD spectroscopy of N-CDs, TiO_2 and TiO_2/N-CDs composite demonstrating successful linking of N-CDs in the lateral sides and in the mesoporous sites

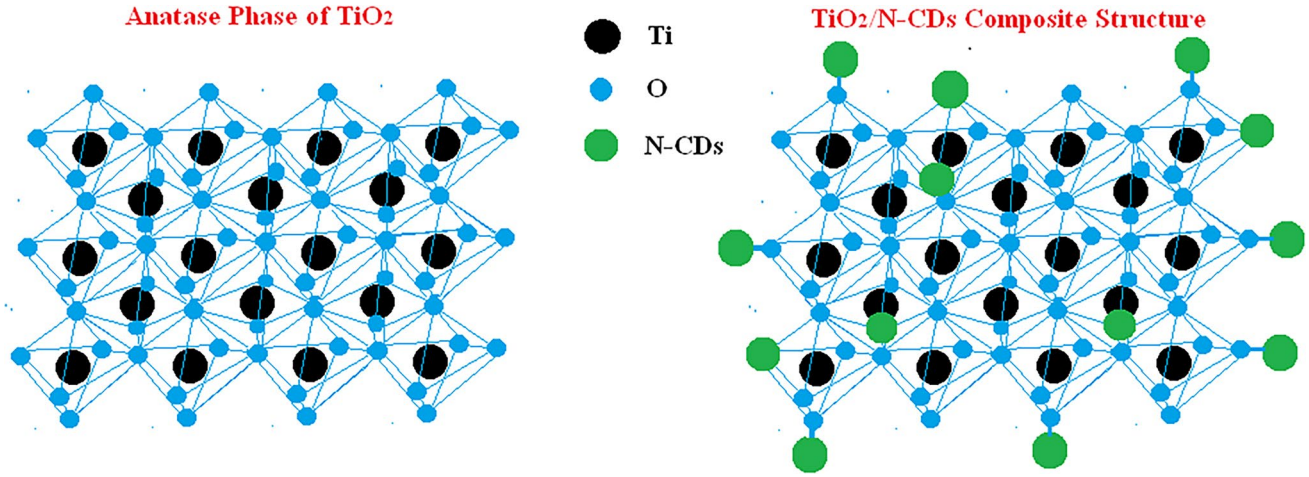

Fig. 4 Systematic structure of anatase phase and TiO_2/N-CDs nano hybrid phase

linked to the edges sites of carbon black (CB) and fills the pore sites and therefore enhances the charge carrier mobility and provides the large active surface area as well as the active sites for the efficient reduction of I_3^-/I^- at the electrolyte/CE interface during the regeneration of dye molecules. Although, agglomerated tridimensional structure of CB/N-CDs composite is shown in Fig. 5.

3.3 *Optical and EIS spectroscopy analysis of TiO_2/N-CDs and CB/N-CDs composite*

We have checked the optical properties of the as prepared TiO_2/N-CDs composite material against pure TiO_2 and N-CDs and the obtained results demonstrated variation in the UV absorption spectrum is shown in Fig. 6a, we have observed from the UV absorption spectroscopy that the absorption spectra shifted towards longer wavelength or shown an increment in the absorption band edge of hybrid TiO_2/N-CDs from pure TiO_2 material moving from 380 to 411 nm associated with the bandgap variation from 3.26 to 3.02 eV which is mainly ascribed to the involvement of newly formed Ti–O–C bond. However, we have also checked the fluorescence emission (PL) of TiO_2 and TiO_2/N-CDs composite at 290 nm excitation wavelength to check the effective electron transport mechanism within the TiO_2/N-CDs composite and have found that after incorporating N-CDs onto the TiO_2 surface the quenching of photo luminescence occurred, this means effective electron transfer has taken place from N-CDs to TiO_2 or defect trapping or surface recombination through non radiative transition/Auger effect/phonon interaction effecting the efficiency of PL emission which is useful for the effective photocatalytic activity towards photocatalytic degradation of environmental toxic dyes proceeded in the current work and the overall quenching of hybrid material can be seen clearly in Fig. 6b.

Further, we have done electrochemical impedance spectroscopy (EIS) to confirm the electron transfer resistance in DSSC's. Figure 7 demonstrated the electrochemical impedance spectra of various DSSC's at open circuit voltage illuminated under AM 1 sun light of 100 mW/cm^{-2} and a frequency range from 0.1 Hz to 100 kHz. Generally, the first gap represents the (Rs) the sheet resistance of FTO glasses and the contact resistance between FTO and TiO_2/N-CDs, FTO and CB/N-CDs material. In addition, three semicircles can be seen in the spectra, the first semicircle in the high frequency side

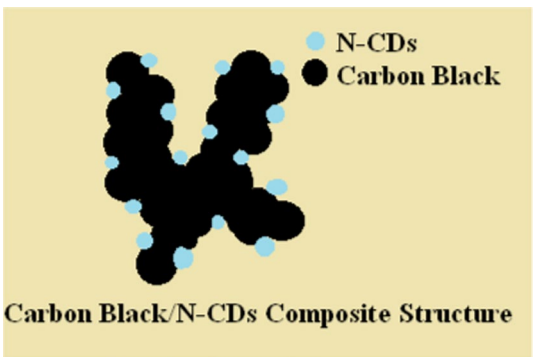

Fig. 5 Agglomerated tridimensional morphology of CB/N-CDs micro composite

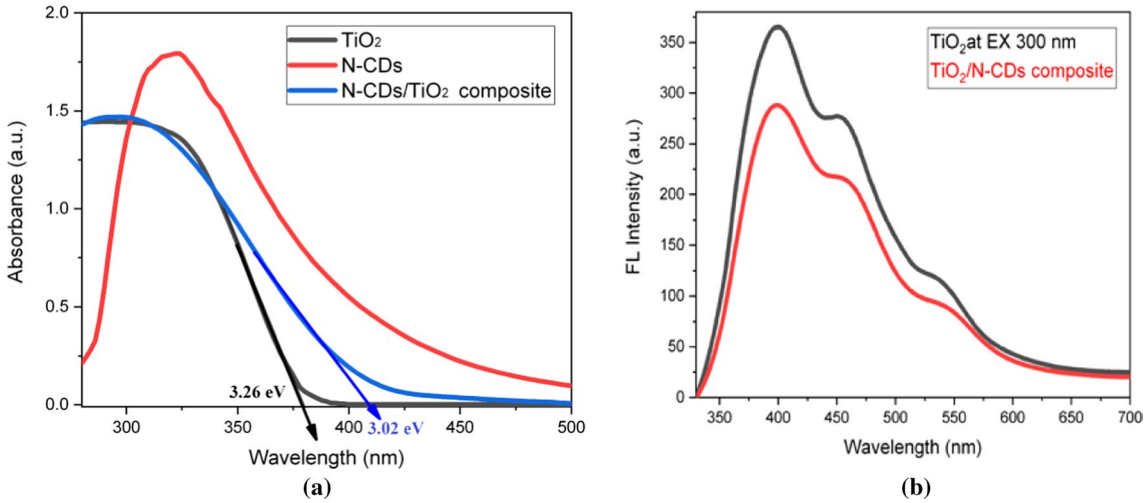

Fig. 6 **a** UV absorption of TiO_2, N-CDs and TiO_2/N-CDs. **b** PL emission of TiO2/N-CDs composite demonstrating non radiative recombination showing effective electron transportation

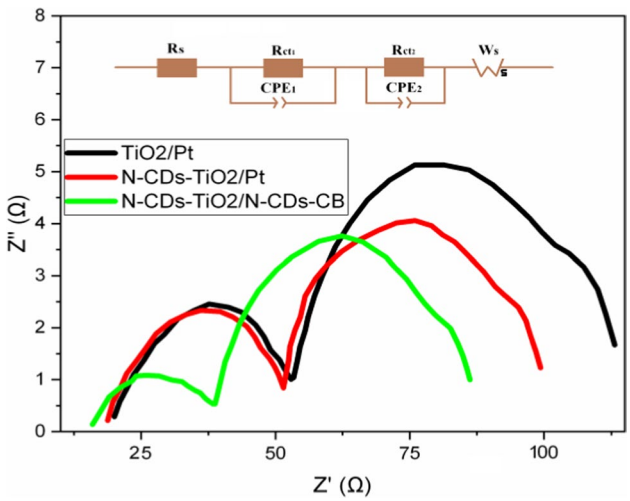

Fig. 7 EIS spectroscopy of various prepared DSSC's

Table 1 Table summarizing the various parameters of EIS spectroscopy of DSSC's

Sample	R_S (Ω)	R_{CE} (Ω)	R_{CT} (Ω)
TiO_2/Pt DSSC	20	52	102
TiO_2/N-CDs/Pt DSSC	19	51	88
TiO_2/N-CDs/CB-N-CDs DSSC	15	38	76

(L.H.S) represented the charge transfer resistance at the electrolyte-counter electrode interface (R_{CE}), the second semicircle represents the charge transfer resistance (R_{CT}) at the electrolyte-TiO_2/N-CDs/dye interface and the third semicircle in the lower frequency side is associated with the characteristics of diffusion of redox electrolyte's (I^-/I_3^-) ionic concentration.

The static resistance R_S (Ω), charge transfer resistance at CE and electrolyte interface R_{CE} (Ω) and charge transfer resistance at photoanode and electrolyte interface R_{CT} (Ω) have been summarized in the Table 1 and based on mentioned data it is clear that the simple conventional DSSC system provided a maximum values of R_S, R_{CE} and R_{CT} as compared with the other two DSSC's indicated that the conventional DSSC offers maximum resistance to the current flow and also demonstrates the maximum recombination effect occurred here, hence decrease in Jsc and overall efficiency. However the second one showed almost the same R_{CE} because of same electrolyte and counter electrode, but reduced R_{CT} because of incorporation of N-CDs into the TiO_2 sample resulted low resistance at interface and low recombination at photoanode hence increased efficiency of cell. While as in third DSSC the both R_{CE} and R_{CT} gets reduced by a considerable factor due

to incorporation of N-CDs in the TiO_2 and replace Pt by CB/N-CDs which possess larger active surface area and enormous active sites due to surface defects for the quick reduction of electrolyte at the CE interface and also by moderate charge transfer mechanism while as in photoanode the N-CDs have broadened the recombination time and blocked the dark current resulted a maximum performance of this novel type of DSSC system for long term usage.

3.4 Photovoltaic study

3.4.1 Modified photo-anode with carbon dots

To ensure proper adhesion between the fluorine doped tin oxide (FTO) glass and the photo anode material and to remove the impurities, the FTO glass slide was first cleaned in a bath sonicator using a soap solution, DI, and Hcl-Ethanol combination (1:10) for 15 min each. Here, the pure TiO_2 and as prepared N-carbon dots were mixed together at the weight ratio of 7:3 in 10 ml of vinegar to reduce the surface tension for the max efficiency of DSSC. The mixture was then ultra-sonicated at 40 kHz for 25 min to form well dispersed slurry and then pasted it on FTO glass using doctor blade method to form a thin layer of this active material approximately 50 µm thick. The photoanode was further heated at 120 °C for 15 min and finally annealed at 500° for 25 min at a heating rate of 5°/min to form a well packed structure of the working electrode with 1 cm^2 surface area, in order to enhance the absorption of TiO_2 in the visible region and effectively separate photogenerated electron–hole pairs. This working electrode was kept in an airtight bag in the dark until further processing.

A simple TiO_2 photo-anode was also prepared by using the above technique for comparison with a modified anode.

3.4.2 Electrochemical activity of carbon dot modified counter electrode

The FTO glass slides were cleaned in an ultrasonic water bath with acetone, ethanol, and de-ionized water and dried in an open air. The FTO glass plate was chosen as the electrode substrate, due to its higher stability, retaining (electrical conductivity, surface roughness and transmittance) compared to ITO glass plates after heat treatment of 450 °C (annealing treatment) because ITO glasses degrade after heat treatment above 350 °C. Form a mixture of the prepared carbon nano composite with carbon black and a binder (PVDF) in the Weight% of 90:5:5 and dispersed in solution of 5 ml pure ethanol and DI water in the ratio of (1:1). To create a well-dispersed suspension, the mixture was ultrasonically treated for 30 min. The as-prepared slurry was applied using the doctor blade technique to the pretreated FTO glass substrate, dried at 80 °C for 15 min in a vacuum oven, and then sintered at 450 °C in the open air for 30 min at a heating rate of 5°/min, and will be used as a counter electrode in the fabrication of DSSC with an effective surface area of 1 cm^2. After that, it was put in an airtight bag for further processing and comparison purposes. Similarly, platinum paste was applied to the conducting glass substrate (FTO) using the doctor blade technique method where thickness was controlled by the use of scotch tape, for creating the reference Pt electrode. The reference Pt electrode was then dried and sintered in an open air at 450 °C for 30 min.

The electro chemical measurements were performed using a potentiostat in an electrochemical cell with three electrodes immersed in an electrolyte solution. Cyclic voltammetry measurements were used to analyse the prepared CE in a three electrode cell with platinum serving as the counter electrode, Ag/AgCl serving as the reference electrode, and one of the constructed CEs serving as the working electrode in 2 M of KOH at a scan rate of 10 mV/s. The results demonstrated that the substantial electrochemical oxidation and reduction peaks are at 0.36 and 0.25 V and further, the −ve slope in the Mott Schottky curve, suggests the relevance of the P type character of produced N-CDs. CV was done in the dark as well as under visible light irradiation at a same scan rate of 10 mV/s, showing an improvement in the photocurrent by approximately 8–9% and has slightly shifted the oxidation peak towards higher potential and reduction peak towards lower potential. The plots of CV and Mott schottky curves are shown in Fig. 8a and b respectively, indicating that this P type CE undergoes both oxidation and reduction and can be utilized in a DSSC solar cell as a counter electrode to replace expensive Platinum as electrode material. The prepared N-CDOTs have bandgap of 2.35 eV as calculated by Tauc plot method and the corresponding band edges (valance and conduction band) are calculated by cyclic voltammetry data set means by E_{onset} reduction (0.31 V) and E_{onset} oxidation (0.32 V) potential. Using formula's (1 and 2), we can easily calculate the band edges, and the calculated valance and conduction band edges are − 4.98 eV and − 2.63 eV.

$$E_{CB} = -\left(E_{ONSET\,OX} + 4.66\right)\,eV \tag{1}$$

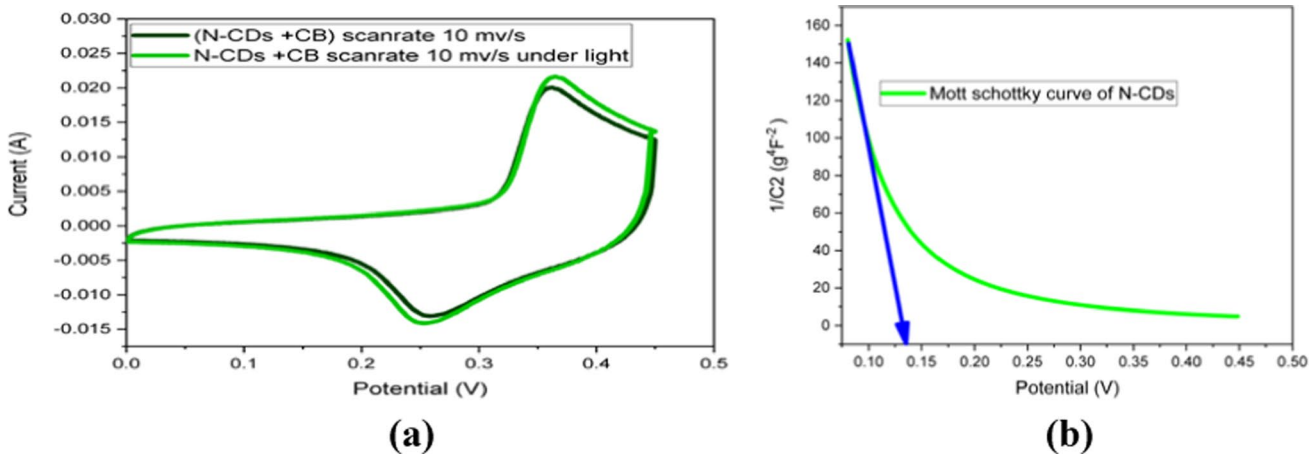

Fig. 8 **a** Cyclic voltagram of N-CDs at 10 mV/s scan rate in dark as well as in visible light irradiation **b** Mott Schottky curve of the N-CDs/CB on NF, illustrating negative slope which shows the P type character of nanomaterial

$$E_{VB} = -\left(E_{CB} - E_g\right). \tag{2}$$

3.4.3 Assembling of DSSC

The sintered modified photo anodes were incubated with Di-tetrabutylammoniumcis-bis -(isothiocyanato) bis (2,2′-bipyridyl-4,4′-dicarboxylato) ruthenium(II) (N719) dye in ethanol solution (0.001 M/L-1) for 24 h. Following the dye's adsorption, the film was cleaned with 100% ethanol to remove any remaining dye and unmoistened in hot air furnace for 24 h at 40 °C. The DSSCs were constructed utilising TiO_2 and TiO_2/N-CDs complex photo-anodes with various counter electrodes (CEs), such as conventional Pt and above mentioned nitrogen doped carbon dot mixed with carbon black CE, independently. The Solaronix thermal polymer spacer (thickness = 100 µm's) was employed between the electrodes to prevent short-circuit by a hot press at 110 °C. Through two tiny holes that were bored on the CE side, polyethylene glycol based I^-/I^{3-} redox electrolyte was pumped into the DSSCs. Surlyn strips were finally used to plug the holes and the resultant active area was 1 cm^2 and the systematic picture of this device is shown in Fig. 9.

3.4.4 Photovoltaic performance of DSSC

The synthesized heteroatom doped N-CQDs + TiO_2 composite was used to prepare dye sensitized solar cells in two different combinations with different counter electrodes (CE): like Platinum and CB + N-CDs, modified CE on FTO glass besides that, another cell with a simple TiO_2 based photoanode and Pt as cathode for reference comparison. In a conventional DSSC system, photogenerated electrons are created by solar radiation, and travelled from the sensitizer dye N719 to the conduction band of TiO_2, and then percolate through TiO_2 to reach the cathode passing

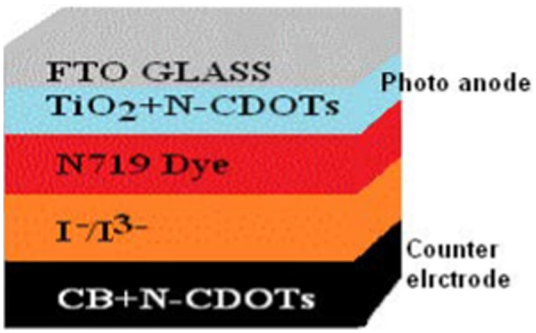

Fig. 9 Schematic diagram of a DSSC solar cell tailored with CCQDs as co-active material in photo anode along with N719 dye and hybrid CB/N-CDs as CE

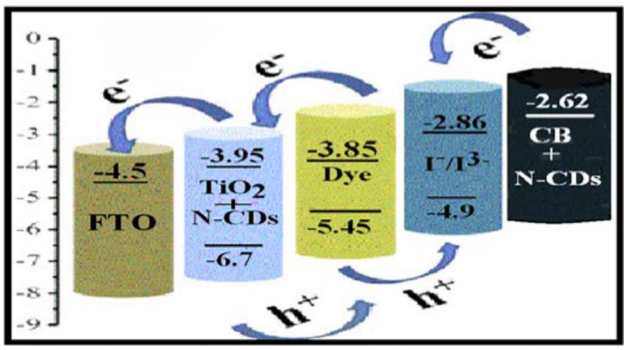

Fig. 10 Energy level diagram showing the favorable influence of N-CDs/TiO_2 as co-active material in the photoanode as well as CB/N-CDs in photocathode and the charge transfer mechanism at both Anode and Cathode

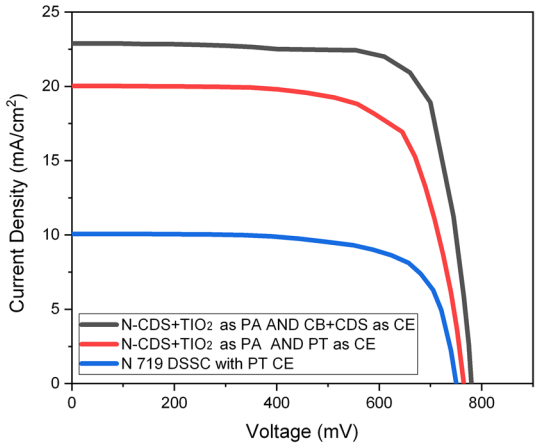

Fig. 11 J–V characteristics of all prepared DSSC's

through FTO glass electrode. To allow electron flow, the band alignment should be positioned appropriately. In the next two configurations, the NCQDs (30%) was used as a co-active material with pure TiO_2 semiconductor material, resulted in a reduced bandgap of photoanode complex from pure TiO_2, lead to an extension of the adsorption band width and covering a larger portion of the visible region of the solar spectrum. This results in a quick extraction of photo-emitted electron from sensitizer dye along with a decreased recombination rate and efficient transfer thereby, enhanced the open circuit voltage (Voc) hence gain in overall photo conversion efficiency of the cell. Further, the carboxylic groups on the N-CDs are firmly affixed to the TiO_2 surface and improved the electron transport mechanism, therefore enhancing photocurrent density. In addition, the prepared N-CDs exhibited excitation dependent photoluminescence behavior, which acted as a secondary source, and broadened the absorption regions towards the UV portion of sun light which in turn lead to a higher photon to electron injection ratio and the enhanced electron transport mechanism of the DSSC device is shown in Fig. 10. However, at the counter electrode the simple Pt based electrode accepts the electron from the external circuit and transferred to the electrolyte for the effective reduction of I^-/I_3^- at the interface during regeneration of sensitizer dye, but the use of CB/N-CDs in counter electrodes works differently, the diffused light inside the cell photo excites the electrons in the valance band of N-CDs and quickly transfers them to the reduction of I^-/I_3^- at the interface besides accepting the electrons from the external circuit, thus reduces the over potential at the interface results lower transfer resistance at the electrolyte and counter electrode proceeded with higher power efficiency. Thus N-CDs acted as a generator and mediator of for transport of mobile charge carriers.

The demonstration of current density versus voltage (J–V) graphs of DSSC shown in Fig. 11, was analyzed during one solar irradiation to assess the cell's photovoltaic abilities, whereas the performance of the fabricated DSSC was measured using a multimeter. It's interesting to note that the N-CDs (acts as a co-active material) combined with TiO_2 as photo anode material along with modified (N-CDs + CB) CE showed more efficiency than a DSSC solely made by TiO_2 and platinum CE. The photoluminescence (PL) caused blue shifting and a depression in the energy bandgap as the N-CDs demonstrated strong absorbance from C=O and C=N transitions following an increase in the amount of C=O and C=N moieties. This boosts light harvesting processes over a wider range of the visible light and created well-distinct charge carriers, and offered a secondary light source to the active material thus, enhanced the photoconversion efficiencies of 13.05% and

10.96% which are 2.5 and 2 times greater than simple TiO_2 based DSSC. Here we have used Eqs. (3) and (4) to compute the devices' fill factors (FF) and photoconversion efficiencies (η) based on the calculated J–V plots.

$$FF = (Jmax \times Vmax)/(Jsc \times Voc) \tag{3}$$

$$\eta = (Jmax \times Vmax)/(Pin \times 100) \tag{4}$$

where Jmax, Vmax, Jsc, Voc and Pin represent the current density, voltage, short-circuit current density, open-circuit voltage and incident light power (100 mW cm^{-2}) respectively.

A number of recent reports and their findings have been summarized in a table form shown in Table 2, in comparison to our present work about improving the efficiency of DSSC against conventional DSSC system. Various procedures have been tried to improve the conventional DSSC system by modifying the photoanode, like adding superior photoactive nano materials to the existing photoactive semiconductor titanium dioxide (TiO_2), in order to harvest maximum portion of sun light into electrical energy and the factors like reducing bandgap, reducing back recombination effect, maximizing absorption band width and recombination time, superior charge generation and transfer mechanism and reducing transfer resistance between the various components of the DSSC system are the key parameters for achieving the desired efficiency of the DSSCs, besides that replacing the conventional platinum (Pt) metal as a cathode material by the carbonous nano materials is also a necessity due to its higher price, rarely found and long term stability issues in the DSSC system for the purpose of achieving maximum potentiality of these solar cells in the long run. According to the previous data, efficiency of DSSC system has been improved after incorporating different photoactive materials to simple base TiO_2 material for instance Singh et al. [90] achieved a power efficiency of 8.80% by incorporating modified TiO_2-rGO-(150 °C) photoanode against TiO_2-pristine GO photo-anode with Pt as cathode with 7.35% power efficiency this is due to the fact of increased photoactive sites, higher effective surface area and better active charge transportation of reduced graphene oxide and titanium dioxide hybrid. In another study, Jahantigh et al. [91] used the single layer graphene quantum dots (SLGQDs)/TiO_2 composite in place of pure TiO_2 as photoanode and achieved a higher photovoltaic performance of 8.92% against 0.12% of pure TiO_2. While as Padmanathan et al. [92] designed and fabricated TiO_2/CDs (5%) as photo anode with Pt as cathode in DSSC system which demonstrated almost 9.21% power efficiency with max FF of 69% against 5.64% of conventional TiO_2 based DSSC system besides that, recently Samir et al. [93] managed to upgrade the conventional photoanode TiO_2 by doping with the nitrogen doped carbon dots and achieved the maximum PCE of 10.87%against

Table 2 A number of recent reports and their findings have been summarized in a table form in comparison to our present work about improving the efficiency of DSSC against conventional DSSC system

DSSC type	J_{SC} (mA/cm^{-2})	V_{OC} (mV)	FF	Efficiency (η) %	References
N-CDs/TiO_2 (anode) and CB/N-CDs (cathode)	22.90	780	0.740	13.22	This work
N-CDs/TiO_2 (anode) and platinum (cathode)	20.00	765	0.724	11.07	This work
TiO_2 (anode) and platinum (cathode)	10.10	750	0.715	5.42	This work
(SLGQDs-N719)/TiO_2 as photoanode and Pt as CE	20.03	730	0.610	8.92	84
TiO_2-N719 as photoanode and Pt as CE	9.30	340	0.410	0.12	84
TiO_2-rGO-150 °C as photoanode and Pt as CE	16.90	739	0.705	8.80	85
TiO_2-pristine GO as photoanode and Pt as CE	13.84	743	0.715	7.35	85
TiO_2/CD (5%) as photoanode and Pt as CE	17.5	710	0.690	9.21	86
TiO_2 as photoanode and Pt as CE	9.2	620	0.680	5.64	86
TiO_2/N-CDs as photoanode and Pt as CE	30.32	1.06	0.338	10.87	87
TiO_2 as photoanode and Pt as CE in N719 dye	28	0.93	0.38	10.10	87
TiO_2/CdS/CdSe as photoanode (10:1) and PbS/CB as CE	13.32	510	0.580	3.91	88
TiO_2/Cds/Cdse as photoanode (10:1) and Pt as CE	10.32	458	0.180	0.85	88
TiO_2/Cds/Cdse as photoanode (10:1) and pure CB as CE	9.87	515	0.390	1.98	88
TiO_2 as photoanode in (N719 dye) and graphene/carbon black (1:3) as CE	15.07	700	0.570	5.99	89
TiO_2 as photoanode in (N719 dye) and Pt as CE	13.35	700	0.650	6.09	89
TiO_2 as photoanode with N719 dye and 8% CB and PVDF (450 °C) as CE	15.01	780	0.720	8.35	90
TiO_2 as photoanode with N719 dye and sputtered Pt as CE	15.19	770	0.710	8.29	90

the conventional bare DSSC which has provided only a PCE 10.10%, in that paper he has also added N-CDs to the N719 sensitizer dye and achieved a PCE of 12.03%, later he tested the same DSSC in diffused and low intensities and acquired max PCE of 18.59% and 24.22% as this is the maximum efficiency until now. But our work has demonstrated an efficiency of 11.07% under 1 sun with a J_{SC} of 20.00 (mA/cm^{-2}) but a considerable amount of output power filfactor (FF) of 72.4% by adding these novel N-CDs to the photoactive TiO_2 sample as photoanode, as this performance is mainly attributed to the higher photoelectron generation with superior charge separation and efficiently transferring them to the conduction band of TiO_2, besides that, the deep trap sites in TiO_2 structure are filled with these N-CDs which are strongly linked to the edge sites of TiO_2 thereby, reducing the band gap, making effective charge transfer process and also reduced the dark current as well. Further the charge transfer resistance has decreased due to the incorporation of these N-CDs in the photoanode, with the electrolyte resulted higher efficiency of this DSSC system.

In addition, the counter electrode needs to be replaced by a cheap and long term stable carbonous nano material for instance Yang et al. [94] replaced Pt counter electrode in high performance quantum dot sensitized solar cell by lead-sulfide and carbon black composite (PbS/CB) and in another same cell platinum is replaced by only CB as counter electrode deposited on the FTO glass and achieved a total photovoltaic performance of 3.91% and 1.98% against platinum based counter electrode DSSC which showed PCE (photoelectric conversion efficiency) of only 0.18%. In another study Pan et al. [95] replaced platinum counter electrode material with graphene-carbon black (1:3) composite and achieved a total PCE of 5.99% against Pt based counter electrode which also showed comparable result of 6.09% but with lower current density and higher FF than former one. In another study Chang et al. [96] mixed carbon black (8–15%) with PVDF pasted on FTO glass as the counter electrode replaced conventional Pt in N719 based DSSC and achieved a maximum PCE of 8.35% against Pt based DSSC system which demonstrated comparable performance of 8.29%. However, in our work we have also replaced the costly and slowly degradable Pt counter electrode by mixing N-CDs with carbon black and a binder PVDF in the percentage ratio of (90:5:5) fabricated on an FTO glass and achieved a total PCE of 13.22% against the Pt based same DSSC, that has demonstrated a total PCE of only 11.07% therefore an improvement of almost 11% in total conversion efficiency, by replacing Pt as a precious and long term degradable material by these cost effective and vastly available novel N-CDs added with CB carbonous material with utmost long term stability, with the iodide/triiodide electrolyte. This is possible only due the effect of efficient transfer of charge carriers, large active surface area, huge no of active sites, photo emitted electron availability, reduced charge transfer resistance and reduced over potential of redox species at electrolyte interface. All these factors have contributed equally and resulted in the overall performance of this novel DSSC system with long term stability against the conventional long term unstable DSSC system in which TiO_2 acted as photo anode and Pt as counter electrode sensitized in N719 dye. Thus we can replace the TiO_2/N-CDs as photoanode and N-CDs/CB as photo cathode replacing TiO_2 and precious Pt with these carbonous nano materials for enhancing the photovoltaic performance of this novel type DSSC system against the conventional DSSC system.

3.4.5 *Advantages and disadvantages of TiO_2/N-CDs composite as photo anode and N-CDs/CB composite as photo cathode in this novel DSSC*

The current research on 3rd generation conventional system technology for dye–sensitized solar cells (DSSC) is going on to improve the power efficiency and the other essential parameters to commercialize the DSSC's globally which are at its early stage now. The current conventional system employs TiO_2 as photo anode and platinum as cathode besides using various other dyes to work as sensitizers. It has been found that the conventional system needs to be replaced by new methods of fabrication technology and by using novel good photo-catalytic materials instead of using only TiO_2 as anode and platinum as cathode which owe various potential draw backs such as fast electron recombination or back electron recombination with the electrolyte and significant electron transfer resistance that have enormously degenerated the performance of DSSC and at the cathode the platinum is slowly oxidised in iodide/triiodide electrolyte thereby destroying its long term stability in addition to that of expensive and rear material. Now our work has provided an alternative pathway/remedy by using TiO_2/N-CDs composite as photo anode and N-CDs/CB composite as photo cathode in dye-sensitized solar cells (DSSC), so that the back recombination effect and significant transfer resistance should be addressed at both the photo anode and at the cathode, thus we have replaced expensive platinum by novel N-CDs/CB composite to provide the long term stability of the cell as well as lower transfer resistance at cathode junction besides the freely available/cheap material. The slow oxidation of platinum metal in the iodide/triiodide electrolyte interface resulted barrier to long term stability of DSSC cell in accordance with the non metallic behavior of N-CDs/carbon black nano complex carbonous material, which have less tendency to react with the electrolyte system, hence maintains the long term stability and performance of DSSC,s.

The advantages and disadvantages of our novel TiO_2/N-CDs composite as photo anode and N-CDs/CB composite as photo cathode in dye-sensitized solar cells (DSSC) is given below:

Advantages:

1. The carbon dots have many enormous merits like intensive quantum yield, low toxicity, simple preparation and easy surface functionalization, so it is economically inexpensive to use these nanomaterials as photoactive materials with various metal oxide materials to increase the photoactive efficiencies of MOS (metal oxide semiconductors). Therefore, the TiO_2/N-CDs nano-composite as photo anode provides sufficient number of surface functional groups and surface active trap sites, which has broadened its UV–Vis absorbance band and red shifted emission band resulting increased performance of DSSC cell in harvesting solar energy at both the ends of DSSC.
2. The N-CDs incorporated in the TiO_2 structure and also in the carbon black helps in tight packing of photoactive material (TiO_2) and carbon black at both the electrode surfaces and also occupy the deep trap sites thus helps in the electron separation and transport mechanism and also avoids the contact between the electrolyte and the FTO glasses at both the ends which causes the corrosion or degradation of FTO glass and also blocks the dark current to flow, results in the overall efficiency of DSSC cell.
3. The heteroatom doping of N-CDs helps in the surface bonding with TiO_2 and reduces the flat band gap of TiO_2 thus absorbs the maximum portion of visible light therefore, promotes the photo excited charge generation and provide large number of transfer paths for electron transport to conduction band of TiO_2 layer and also enhances the forward reduction reaction thereby minimizing the photoluminescence intensity of the composite material as can be seen in the emission spectra of composite material and extends the lifetime of excited electrons which decreases the recombination rate of electron hole pairs and therefore provides the higher short circuit current density, open circuit voltage and thus enhances the corresponding power generating efficiency of DSSC.
4. In both the electrodes the N-CDs acts as charge donor and mediator for quick transfer of charge carriers upon absorbing visible light and reduced the over potential at both the electrode electrolyte interfaces which has decreased the charge transfer resistance as compared to conventional TiO_2/Pt based DSSC and hence increase in the efficiency of DSSC. The efficiency of DSSC with this modified photoanode and photo cathode was 13.22% with Voc, Jsc and FF of 0.780 V, 22.90 mA/cm^2 and 0.74 values and efficiency of the DSSC based on modified anode TiO_2/N-CDs and Pt cathode was 11.07% with Voc, Jsc and FF of 0.765 V, 20 mA/cm^2 and 0.724 against the conventional DSSC based on TiO_2 as anode and Pt as conventional counter electrode was 5.42% giving open circuit voltage and current density of 0.750 V and 10.10 mA/cm^2 while as FF is only 0.715. The results demonstrated that modified photo electrode and Pt based DSSC provides almost 2 times higher performance than simple conventional DSSC as prepared, which is mainly understood by charge generation and extraction due to incorporation of N-CDs into the TiO_2 photoanode. However, the DSSC with both the modified electrodes demonstrated almost 2.5 fold increase in power efficiency as compared to conventional DSSC this is because of the fact that upon absorption of photons at counter electrode by nitrogen doped carbon dots thereby, reduces the over potential for reduction of I_3^- to I^- at the electrode and electrolyte interface which has also reduced the charge transfer resistance at the interface thus they acted as both generators and donors of charge carriers resulted more efficiency of DSSC.
5. The variation of charge transfer resistance by these N-CDs incorporated in TiO_2 as modified photo anode and carbon black as modified cathode are demonstrated by EIS spectroscopy are 75Ω and 38Ω at photo anode and counter electrode with the redox electrolyte against the conventional DSSC showing 104 Ω and 53 Ω.

Disadvantages:

1. The electron density increases as the concentration of redox electrolyte, but as the concentration increases the electrolyte breaks to diiodide radicals by light absorption as the N-CDs are hydrophilic in nature however they provide a blocking layer for back electron recombination but the hydrophilic character of N-CDs does not provide a full blocking of back electron recombination, so to avoid such abnormality the cardon dots should be hydrophobic in nature.
2. The loss of electrolyte by leaking causes the degradation of solar cell and decreases active surface area of DSSC cell hence reduction in efficiency and needs refilling periodically, in order to avoid such a loss the gel type electrolyte should be used.

3. At the cathode the N-CDs/CB deposited on FTO glass acts as modified cathode and works well however the optimal ratio between carbon dots and carbon black can be challenging and affects the electron transport and charge collection efficiency.
4. The carbon dots used as photoanode and as photocathode is at its early stage now, so long term stability issues could be a challenging question towards the long term performance of DSSC's, to remove that ambiguity a sophisticated method of fabrication of these N-CDs at both the electrode surfaces.
5. The use of TCO glass shall be preferred against ITO and FTO glasses because the former provides both the long term chemical stability and lower sheet resistance (0.5Ω) against harsh operating conditions as compared to the latter two.
6. The use of sealant materials to seal the DSSC cell against leakage as their sealing capability decreases with temperature variation and pressure developed inside. To avoid such an abnormality a sealant should be produced that will be strongly bonded with the glass electrodes.

3.5 Degradation of MB

3.5.1 *Preparation of modified self-heteroatom doped N-CDs/TiO_2 hybrid photo-catalyst*

Initially, 30 ml of DI water was used to disperse 1 g of TiO_2 powder and 500 mg of previously synthesised heteroatom doped carbon dots in the ratio of 2:1. A well-dispersed suspension was then obtained by ultrasonically processing the combination for 30 min at a frequency of 40 kHz in an ultrasonic bath. To acquire the necessary photocatalyst, this solution was transferred to a glass beaker and micro-waved at 900 W for 5 min, then the final product was centrifuged at 5000 rpm, and washed with DI water and ethanol three to four times, further dried at 70 °C in an oven for 24 h. Then, the photocatalyst was sealed in a bag and stored in dark place for further processing.

3.5.2 *Photocatalytic activity of heteroatom doped N-CQDs/TiO_2 hybrid nanocomposite*

Under UV illumination from a mercury lamp with a wavelength of 254 nm, towards the photocatalytic degradation of Methylene blue by heteroatom doped CDs/TiO_2 composite material was carried out, as a consequence of the multi heteroatom doping, enormous active redox sites and good fluorescence performance of the composite. Herein, the highest performance of the amalgam of TiO_2 and heteroatom doped N-CDs (TiO_2/N-CDs) was explored as a photo-catalyst for the UV degradation of MB. Here we have used 100 mg of the hybrid photocatalyst mixed with 100 mg/L of MB in a glass beaker. The mixture was then dissolved for 10 min before incubating it for 24 h at room temperature, until full adsorption desorption of dye molecules took place. For comparison purposes the hybrid photocatalyst was replaced with N-CDs and the same steps were followed. These solutions were taken individually and kept under UV (254 nm) LED light for approximately 18 min, and 1/3 of the sample was taken every 6 min for photo absorbance measurement and the results are shown in Fig. 12a, b after irradiation take place towards photo-degradation of MB. Only one measurement was performed after 18 min with the reference catalyst N-CDs.

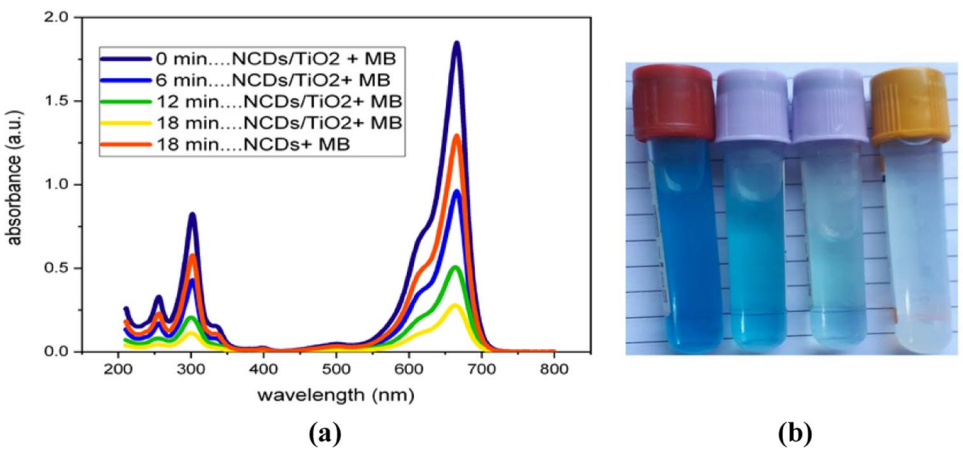

Fig. 12 **a** UV absorbance of MB with short UV irradiation time in presence of N-CDs and hybrid TiO_2/N-CDs photocatalyst **b** discoloration of MB due to photocatalytic activity of N-CDs/TiO_2

From the results shown, it is clear that the prepared heteroatom doped carbon dots degraded the MB to only 30%, but, the TiO_2-N-CDs nanocomposite showed higher degrading performance of 85% after 18 min of short UV irradiation period, which is approximately 2–3 times higher that of reference N-CDs. TiO_2 nanoparticles and NSP-CDs have worked together synergistically to increase the photocatalytic activity of TiO_2/N-CDs. In accordance with the electrochemical activity of hetero atom doped N-CDs, the heteroatom contained functional groups in N-CDs resulted in rich edges, high-density redox-active centres, and defects and have the potential to increase overall catalytic activity by transferring the photoexcited electrons from TiO_2 to N-CDs henceforth, minimizes the recombination of electrons and holes.

In order to fully understand the photocatalytic capability, the photo-degradation and reaction degradation kinetics are illustrated in Fig. 13a, b, which clearly demonstrate pseudo-first order kinetics: $-\ln(C/C_0) = kt$, where k (min^{-1}) is rate constant, and t (min) is the irradiation time. The degrading reaction rate constants k_1 and k_2, clearly indicated that Pure N-CDs as photocatalyst has a low $k_1 = (0.020\ min^{-1})$ as compared with the hybrid N-CDs/TiO_2 nanocomposite which showed a maximum of $k_2 = (0.1068\ min^{-1})$ and hence demonstrated an outstanding performance rather than pure N-CDs as catalyst.

Heteroatom doped N-CDs, a P-type semiconductor as demonstrated by the electrochemical activity discussed above and the Fermi level of N-CDs is lower than TiO_2 which caused the electrons to diffuse from the N-CDs to the TiO_2 until the two Fermi levels are balanced as soon as the N-CDs were deposited onto the TiO_2 edges, which resulted in the creation of a p–n junction and a built-in electric field E from TiO_2 towards the N-CDs and also caused the N-CDs energy band to shift upward thereby reducing the gap difference. The photodegradation process started as soon as the short UV light excited the N-CDs/TiO_2 hybrid photoanode. The nanohybrids responded through the creation of photogenerated carriers and the holes collected on the VB of TiO_2 continue to migrate towards the VB of the N-CDs, while as the photoinduced electrons in the CB of the N-CDs migrate to the CB of TiO_2, driven by the p–n junction's inherent electric field and hence further reduced the energy level difference between the N-CDs and TiO_2. Therefore inhibiting direct recombination of the photogenerated electron–hole pairs, while as the electric field efficiently and quickly transferred the photogenerated carriers, leaving the free charges fully engaged in the oxidation process of the dye molecules and hence, accelerating the pollutant degradation. It is a well known fact that photogenerated electrons in the CB have the ability to form $\cdot O_2^-$ and the photogenerated holes on the VB can oxidise water to produce $\cdot OH^-$ radicals, both of which are essential for the breakdown of dye molecule structures and can be seen in Fig. 14, these active species eventually converted the dye molecules to CO_2 and H_2O. Thus the complex of N-CDs/TiO_2 complex behaves a good photocatalyst for degradation of environmental toxic dyes.

The prepared N-CDs contain various doping agents such as nitrogen, oxygen and carbon in bulk quantity as discussed already but fewer percentage of other elements like phosphorus, sulpher and zinc that have provided rich active sites and surface dislocations that will help in the efficient electron transport for the degradation of toxic dyes. However, various N-CDs systems have been already tested with varying doping percentages of different elements for the degradation of dyes. Table 3 has summarized the efficiencies of different N-CDs in TiO_2 photoactive material system for comparison purposes with this present work: the comparative analysis between various carbon dot systems mixed with pure TiO_2 showed different degradation rate constants against the various organic compounds and dyes [97–103]. However, the pure TiO_2 thin film as a solo photocatalyst has been recently reported in (2023) with reference number [104] demonstrated

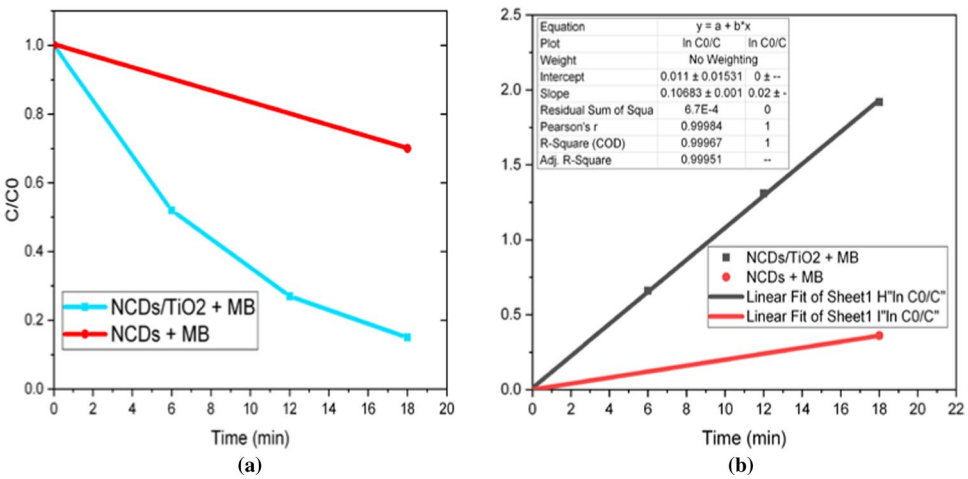

Fig. 13 **a** Rate of photo-degradation of MB due to N-CDs/TiO_2 nanocomposite **b** photo-degradation kinematics demonstrating first order kinetics with high rate constant of N-CDs/TiO_2 nanocomposite as compared to only N-CDs photocatalyst

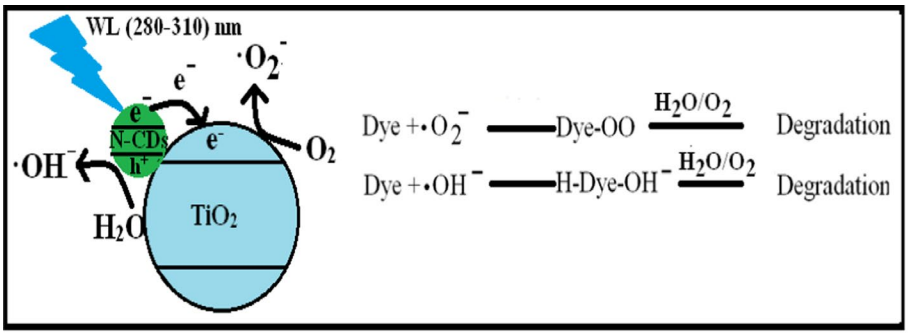

Fig. 14 Mechanism of photo degradation of azo dyes

Table 3 This table has summarized the efficiencies of different N-CDs in TiO_2 photoactive material system for comparison purposes with our present work

Catalyst/dye	Light/rate constant	Time (min)/degradation %	References
NCQDS/TNSs@Cu_2O/methyl orange	Visible light/0.1062	60/99	[97]
N-GQDs/TiO_2/methylene blue	UV (400 nm)/-	17/85	[98]
N-CDs/TiO_2/MB	UV/0.0593	40/90	[99]
TiO_2/CQDs/MB	Visible light/0.2054	10/100	[100]
CQDs-x/TiO_2/organic compounds	Visible light/–	–	[101]
CQDs/TiO_2/MB	UV/0.0365	10/80	[102]
CQDs/TiO_2/RhB	Visible Light	30/85.47	[103]
TiO_2 thin film/MB	UV/-	300/20	[104]
N-CDs/TiO_2/MB	UV/0.1068	18/85	This work
N-CDs/MB	UV/0.020	18/30	This work

photocatalysis of MB and degraded only 20% of methylene blue in 300 min, but our work has demonstrated 85% degradation of MB in only 18 min of irradiation time and the highest degradation rate constant, because of the efficient hydrolysis of water thus, produced reactive oxygen species and H^+ ions that have catalyzed the dye molecules more efficiently and deteriorated the dye molecules by the process of efficient transfer between N-CDs and TiO_2 due to their varying band positions.

4 Conclusions and future work

This work has examined a general overview of green, microwave irradiated process for production of heteroatom-doped N-carbon dots from pumpkin seeds, which has been recently published by us associated with the variety of characterization techniques, including UV–Vis absorption, fluorescence spectroscopy, X-ray diffraction (XRD), scanning electron microscopy (SEM), Fourier transform infrared spectroscopy (FT-IR), and energy dispersive X-ray spectroscopy (EDX). However, a number of essential benefits have been accessed with this one-step synthesis method: it is straightforward, economical, efficient, fast production and yields amazing fluorescence quantum yield of 65.50%. Herein, the present study of modified TiO_2 with N-CDs based photoanode along with the modified CB/N-CDs CE exhibited an overall efficiency of 250% in accordance with the simple TiO_2/N719 DSSC under one sun, and will contribute towards development of solar cell technology. Further, under short UV 25 nm illumination, the N-CDs have further enhanced TiO_2's photocatalytic activity for the disintegration of methylene blue within only 18 min of exposure time, deteriorated 85% of the MB. Thus this novel nanomaterial has enormous scope towards the future of this planet.

We have assembled the novel DSSC replacing conventional DSSC system in which we have replaced both the photoanode and cathode by photocathode to maximize the power efficiency of this solar cell and we succeeded to do this but the power efficiency is not so enough that it can be used commercially, so it needs future directions and also indentify the challenges in attaining the long term active usage and accessing considerable efficiency in the near future for their promising perspectives.

Future directions for DSSC:

- Efficiency improvements: Efficiency can be improved by the use of non toxic organic dyes that absorb most part of sun light including the UV and infrared part, besides this, the materials used in photoanode and at counter electrode needs to be optimised for better efficiency of DSSC. In addition to this the architecture needs to be optimised or replaced by new fabrication methods.
- Stability issues: The DSSC's needs to be more stable and durable for their long term performance especially in harsh environmental conditions.
- Scalability and cost reduction: The need for novel manufacturing techniques that allow large scale production of these DSSC's at lower costs will enable commercial viability.

Challenges facing DSSC's:

- Efficiency limitations: The DSSC's offer several advantages like low cost fabrication and flexibility but their efficiency is lower as compared to that of silicon-based solar cells etc.
- Stability issues: The DSSC's have certain issues like electrolyte leakage, dye degradation and electrode corrosion, therefore limiting their long term stability and reliability.
- Material availability: The DSSC's system needs some precious and rare materials like ruthenium based dyes and some electrolytes that have certain environmental issues, demanding new alternative materials.

Promising perspectives:

- The perspectives of DSSC's are framed by their convenience and ongoing research work. They should be flexible and versatile for their use in wearable devices, portable devices.
- Low cost fabrication and low light performance for indoor and cloudy environments
- They should support tuning properties to work in different environmental conditions and are environmentally sustainable.
- The AI should be used to provide new fabrication techniques and in finding new photoactive stable materials that offer promising development of high performance DSSC's.

Acknowledgements I would like to extend my gratitude to Govt Degree College for Women Anantnag, NIT Srinagar and Bhagwant University, Ajmer for their support in providing resources, infrastructure and immeasurable moral support in this endeavor. I wish to dedicate this research work paper to my parents Bashir Ahmad and Dilshada Bano and my brothers and sisters especially my wife and daughter Yasmeena and Aisha Abdullah who have always been an endless source of inspiration and joy in my life.

Author contributions MAS: Conceptualization, manuscript composition, data curation, methodology, experimentation, investigation, validation, writing original draft, formal analysis and visualization. RSC: supervision. KA: review and editing, validation and visualization.

Funding No overall funding for this work.

Data availability The datasets generated during and/or analysed during the current study are available from the corresponding author on reasonable request.

Declarations

Competing interests The authors declare no competing interests.

Ethics approval Not applicable.

Open Access This article is licensed under a Creative Commons Attribution 4.0 International License, which permits use, sharing, adaptation, distribution and reproduction in any medium or format, as long as you give appropriate credit to the original author(s) and the source, provide a link to the Creative Commons licence, and indicate if changes were made. The images or other third party material in this article are included in the article's Creative Commons licence, unless indicated otherwise in a credit line to the material. If material is not included in the article's Creative Commons licence and your intended use is not permitted by statutory regulation or exceeds the permitted use, you will need to obtain permission directly from the copyright holder. To view a copy of this licence, visit http://creativecommons.org/licenses/by/4.0/.

References

1. Sukhorukov G, Goryacheva I, Sapelkin A. Carbon nanodots: mechanisms of photoluminescence and principles of application. Trends Anal Chem. 2017;90:27–37.
2. Sun X, Lei Y. Fluorescent carbon dots and their sensing applications. Trends Anal Chem. 2017;89:163–80.
3. Zhang J, Yu S-H. Carbon dots: large-scale synthesis, sensing and bioimaging. Mater Today. 2016;19(7):382–93.
4. Sciortino A, Cannizzo A, Messina F. Carbon nanodots: a review—from the current understanding of the fundamental photophysics to the full control of the optical response. C. 2018;4(4):67.
5. Yuan F, et al. Shining carbon dots: synthesis and biomedical and optoelectronic applications. Nano Today. 2016;11(5):565–86.
6. Namdari P, Negahdari B, Eatemadi A. Synthesis, properties and biomedical applications of carbon-based quantum dots: an updated review. Biomed Pharmacother. 2017;87:209–22.
7. Arcudi F, Strauss V, Đorđević L, Cadranel A, Guldi DM, Prato M. Angew Chem Int Ed. 2017;129:12265.
8. Sun Z, Li X, Wu Y, Wei C. Zeng New J Chem. 2018;42:4603.
9. Xu XY, Ray R, Gu YL, Ploehn HJ, Gearheart L, Raker K, Scrivens WA. Electrophoretic analysis and purification of fluorescent single-walled carbon nanotube fragments. J Am Chem Soc. 2004;126:12736–7.
10. Sun YP, Bing Z, Yi L, Wei W, Fernando KAS, Pathak P, Meziani MJ, Harruff BA, Xin W, Wang H. Quantum-sized carbon dots for bright and colorful photoluminescence. J Am Chem Soc. 2006;128:7756–7.
11. Zhang MR, Su R, Zhong J, Fei L, Cai W, Guan QW, Li WJ, Li N, Chen YS, Cai LL. Red/orange dual-emissive carbon dots for pH sensing and cell imaging. Nano Res. 2019;12:815–21.
12. Zhang YN, Zhang XW, Shi YP, Sun C, Zhou N, Wen HX. The synthesis and functional study of multicolor nitrogen-doped carbon dots for live cell nuclear imaging. Molecules. 2020;25:306.
13. Liu JJ, Dong YY, Ma YX, Han YX, Ma S, Chen HL, Chen XG. One-step synthesis of red/green dual-emissive carbon dots for ratiometric sensitive ONOO− probing and cell imaging. Nanoscale. 2018;10:13589–98.
14. Qin KH, Zhang DF, Ding YF, Zheng XD, Xiang YY, Hua JH, Zhang Q, Ji XL, Li B, Wei YL. Applications of hydrothermal synthesis of *Escherichia coli* derived carbon dots in in vitro and in vivo imaging and p-nitrophenol detection. Analyst. 2020;145:177–83.
15. Liu JJ, Li DW, Zhang K, Yang MX, Sun HC, Yang B. One step hydrothermal synthesis of nitrogen-doped conjugated carbonized polymer dots with 31% efficient red emission for in vivo imaging. Small. 2018;14:1703919–29.
16. Shu Y, Lu J, Mao QX, Song RS, Wang XY, Chen XW, Wang JH. Ionic liquid mediated organophilic carbon dots for drug delivery and bioimaging. Carbon. 2017;114:324–33.
17. Kailasa SK, Bhamore JR, Koduru JR, Park TJ. Carbon dots as carriers for the development of controlled drug and gene delivery systems. In: Grumezescu AM, editor. Biomedical applications of nanoparticles. Amsterdam: Elsevier; 2019. p. 295–317.
18. Yang T, Huang JL, Wang YT, Zheng AQ, Shu Y, Wang JH. β-cyclodextrin-decorated carbon dots serve as nanocarriers for targeted drug delivery and controlled release. ChemNanoMat. 2019;5:479–87.
19. Jana J, Lee HJ, Chung JS, Kim MH, Hur SH. Blue emitting nitrogen-doped carbon dots as a fluorescent probe for nitrite ion sensing and cell-imaging. Anal Chim Acta. 2019;1079:212–9.
20. Wang J, Li RS, Zhang HZ, Wang N, Zhang Z, Huang CZ. Highly fluorescent carbon dots as selective and visual probes for sensing copper ions in living cells via an electron transfer process. Biosens Bioelectron. 2017;97:157–63.
21. Hu J, Tang F, Jiang Y, Liu C. Rapid screening and quantitative detection of Salmonella using a quantum dot nanobead-based biosensor. Analyst. 2020;145:2184–90.
22. Han M, Zhu SJ, Lu S, Song YB, Feng TL, Tao SY, Liu JJ, Yang B. Recent progress on the photocatalysis of carbon dots: classification, mechanism and applications. Nano Today. 2018;19:201–18.
23. Yu HJ, Shi R, Zhao YF, Waterhouse GI, Wu LZ, Tung CH, Zhang TR. Smart utilization of carbon dots in semiconductor photocatalysis. Adv Mater. 2016;28:9454–77.
24. Zhou Y, Zahran EM, Quiroga BA, Perez J, Mintz KJ, Peng Z, Liyanage PY, Pandey RR, Chusuei CC, Leblanc RM. Size-dependent photocatalytic activity of carbon dots with surface-state determined photoluminescence. Appl Catal B. 2019;248:157–66.
25. Yuan FL, Yuan T, Sui LZ, Wang ZB, Xi Z, Li YC, Li XH, Fan LZ, Tan ZA, Chen A, et al. Engineering triangular carbon quantum dots with unprecedented narrow bandwidth emission for multicolored LEDs. Nat Commun. 2018;9:2249–60.
26. Zheng JX, Liu XH, Yang YZ, Liu XG, Xu BS. Rapid and green synthesis of fluorescent carbon dots from starch for white light-emitting diodes. New Carbon Mater. 2018;33:276–88.
27. Hu C, Li MY, Qiu JS, Sun YP. Design and fabrication of carbon dots for energy conversion and storage. Chem Soc Rev. 2019;48:2315–37.
28. Fernando KS, Sahu S, Liu Y, Lewis WK, Guliants EA, Jafariyan A, Wang P, Bunker CE, Sun YP. Carbon quantum dots and applications in photocatalytic energy conversion. ACS Appl Mater Interfaces. 2015;7:8363–76.
29. Genc R, Alas MO, Harputlu E, Repp S, Kremer N, Castellano M, Colak SG, Ocakoglu K, Erdem E. High-capacitance hybrid supercapacitor based on multi-colored fluorescent carbon-dots. Sci Rep. 2017;7:11222.
30. Huang HY, Cui Y, Liu MY, Chen JY, Wan Q, Wen YQ, Deng FJ, Zhou NG, Zhang XY, Wei Y. A one-step ultrasonic irradiation assisted strategy for the preparation of polymer-functionalized carbon quantum dots and their biological imaging. J Colloid Interface Sci. 2018;532:767–73.
31. Qiao ZA, Wang YF, Gao Y, Li HW, Dai TY, Liu YL, Huo QS. Commercially activated carbon as the source for producing multicolor photoluminescent carbon dots by chemical oxidation. Chem Commun. 2010;46:8812–4.
32. Zheng H, Wang Q, Long Y, Zhang H, Huang X, Zhu R. Enhancing the luminescence of carbon dots with a reduction pathway. Chem Commun. 2011;47:10650–2.
33. Liu H, Li Z, Sun Y, Geng X, Hu Y, Meng H, Ge J, Qu L. Synthesis of luminescent carbon dots with ultrahigh quantum yield and inherent folate receptor-positive cancer cell targetability. Sci Rep. 2018;8:1086.
34. Yarur F, Macairan JR, Naccache R. Ratiometric detection of heavy metal ions using fluorescent carbon dots. Environ Sci. 2019;6:1121–30.

35. Yu D, Nagelli E, Du F, Dai L. J Phys Chem Lett. 2010;1:2165–73.
36. Nazeeruddin MK, Kay A, Rodicio I, Humphry-Baker R, Müller E, Liska P, Vlachopoulos N, Graetzel M. Conversion of light to electricity by cis-X2bis(2,2′-bipyridyl-4,4′-dicarboxylate) ruthenium(II) charge-transfer sensitizers (X=Cl–, Br–, I–, CN–, and SCN–) on nanocrystalline TiO electrodes. J Am Chem Soc. 1993;8:6382–90.
37. Hagfeldt A, Grätzel M. Molecular photovoltaics. Acc Chem Res. 2000;8:269–77.
38. Grätzel M. Photo electrochemical cells. Nature. 2001;8:338–44.
39. Lim J, Lee M, Balasingam SK, Kim J, Kim D, Jun Y. Fabrication of panchromatic dye-sensitized solar cells using pre-dye coated TiO2 nanoparticles by a simple dip coating technique. RSC Adv. 2013;8:4801–5.
40. Ali FH, Alwan DB. Effect of particle size of TiO_2 and additive materials to improve dye sensitized solar cells efficiency. J Phys. 2018;1003:012077.
41. Kumar S, Pradhan S, Dhar A. Enhanced performance with the incorporation of organo-metal trihalide perovskite in nanostructured ZnO solar cell. Proc Eng. 2016;141:1–6.
42. Wang F, Zhang Y, Yang M, Du J, Yang L, Fan LS, Sui Y, Liu X, Yang J. Achieving efficient flexible perovskite solar cells with room-temperature processed tungsten oxide electron transport layer. J Power Sources. 2019;440:227157.
43. Dao V-D, Larina LL, Lee J-K, Jung K-D, Huye BT, Choi H-S. Graphene-based RuO_2 nanohybrid as a highly efficient catalyst for triiodide reduction in dye-sensitized solar cells. Carbon. 2015;81:710–9.
44. Guo X, Di W, Chen C, Wang X, Qin W. Enhanced near-infrared photocatalysis of NaYF4:Yb, Tm/CdS/TiO_2 composites. Dalton Trans. 2014;43:1048–54.
45. Khan SU, Al-Shahry M, Ingler WB. Efficient photochemical water splitting by a chemically modified n-TiO_2. Science. 2002;297:2243–5.
46. Tian J, Zhao Z, Kumar A, Boughton RI, Liu H. Recent progress in design, synthesis, and applications of one-dimensional Ti O2 nanostructured surface heterostructures: a review. Chem Soc Rev. 2014;43:6920–37.
47. Seger B, McCray J, Mukherji A, Zong X, Xing Z, Wang L. An n-type to p-type switchable photoelectrode assembled from alternating exfoliated titania nanosheets and polyaniline layers. Angew Chem Int Ed. 2013;52:6400–3.
48. Wang X, Li Z, Shi J, Yu Y. One-dimensional titanium dioxide nanomaterials: nanowires, nanorods, and nanobelts. Chem Rev. 2014;114:9346–84.
49. Nanomaterials. 2017;7:130. https://doi.org/10.3390/nano7060130.
50. https://doi.org/10.1016/j.carbon.2021.06.090.
51. Paulo S, Palomares E, Martinez-Ferrero E. Graphene and carbon quantum dot-based materials in photovoltaic devices: from synthesis to applications. Nanomaterials. 2016;6:157.
52. Narayanan R, Deepa M, Srivastava AK. Förster resonance energy transfer and carbon dots enhance light harvesting in a solid-state quantum dot solar cell. J Mater Chem A. 2013;1:3907–18.
53. Xu H, Duan J, Zhao Y, Jiao Z, He B, Tang Q. 9.13%-efficiency and stable inorganic CsPbBr 3 solar cells. Lead-free CsSnBr3-XIx quantum dots promote charge extraction. J Power Sources. 2018;399:76–82.
54. Xu H, Yuan H, Duan J, Zhao Y, Jiao Z, Tang Q. Lead-free CH3NH3SnBr 3-XIx perovskite quantum dots for mesoscopic solar cell applications. Electrochim Acta. 2018;282:807–12.
55. Duan J, Zhao Y, He B, Jiao Z, Tang Q. Controllable synthesis of organic-inorganic hybrid halide perovskite quantum dots for quasi-solid-state solar cells. Electrochim Acta. 2018;282:263–9.
56. Griffini G, Bella F, Nisic F, Dragonetti C, Roberto D, Levi M, Bongiovanni R, Turri S. Multifunctional luminescent down-shifting fluoropolymer coatings: a straightforward strategy to improve the UV-Light harvesting ability and longterm outdoor stability of organic dye-sensitized solar cells. Adv Energy Mater. 2015;5:1401312.
57. Grätzel M. J Photochem Photobiol C Photochem Rev. 2003;4:145–53.
58. Xu T, Wei P, Ren X, Liu H, Chen L, Tian W, Liu S, Guo Z. Mater Lett. 2017;195:100–3.
59. He H, Zhang C, Liu T, Cao Y, Wang N, Guo Z. J Mater Chem A. 2016;4:9362–9.
60. Papageorgiou N, Maier W, Grätzel M. J Electrochem Soc. 1997;144:876–84.
61. Papageorgiou N. Coord Chem Rev. 2004;248:1421–46.
62. Fang X, Ma T, Guan G, Akiyama M, Kida T, Abe E. J Electroanal Chem. 2004;570:257–63.
63. Yang C-C, Zhang HQ, Zheng YR. Curr Appl Phys. 2011;11:S147–53.
64. Lee WJ, Ramasamy E, Lee DY, Song JS. Sol Energy Mater Sol Cells. 2008;92:814–8.
65. Olsen E, Hagen G, Lindquist S. Sol Energy Mater Sol Cells. 2000;63:267–73.
66. Chen L, et al. Graphene quantum-dot-doped polypyrrole counter electrode for high-performance dye-sensitized solar cells. ACS Appl Mater Interfaces. 2013;5(6):2047–52.
67. Chen H, Hao L, Li T, Gao L, He H, Wang N, Guo Z. J Mater Chem A. 2017;1:1. https://doi.org/10.1039/C7TA05123A.
68. Murugadoss V, Wang N, Tadakamalla S, Wang B, Guo Z, Angaiah S. J Mater Chem A. 2017. https://doi.org/10.1039/C7TA00941K.
69. Smestad G, Bignozzi C, Argazzi R. Sol Energy Mater Sol Cells. 1994;32:259–72.
70. Murakami TN, Grätzel M. Inorg Chim Acta. 2008;361:572–80.
71. Chen J, Yan Y, Lin K. J Chin Chem Soc. 2010;57:1180–1.
72. Kim J-M, Rhee S-W. Electrochim Acta. 2012;83:264–70.
73. Zhang J, Wu Y, Xing M, Leghari SAK, Sajjad S. Development of modified N doped TiO2 photocatalyst with metals, nonmetals and metal oxides. Energy Environ Sci. 2010;3:715–26.
74. Chong MN, Jin B, Chow CW, Saint C. Recent developments in photocatalytic water treatment technology: a review. Water Res. 2010;44(10):2997–3027.
75. Kubacka A, Fernandez-Garcia M, Colon G. Advanced nanoarchitectures for solar photocatalytic applications. Chem Rev. 2012;112(3):1555–614.
76. Atchudan R, Jebakumar Immanuel Edison TN, Perumal S, Karthikeyan D, Lee YR. Effective photocatalytic degradation of anthropogenic dyes using graphene oxide grafting titanium dioxide nanoparticles under UV-light irradiation. J Photochem Photobiol A. 2017;333:92–104.

77. Wang JL, Xu LJ. Crit Rev Environ Sci Technol. 2012;42(3):251–325. https://doi.org/10.1080/10643389.2010.507698.
78. Safardoust-Hojaghan H, Salavati-Niasari M. Degradation of methylene blue as a pollutant with N-doped graphene quantum dot/titanium dioxide nanocomposite. J Clean Prod. 2017;148:31–6.
79. Nuengmatcha P, Chanthai S, Mahachai R, Oh WC. Sonocatalytic performance of ZnO/graphene/TiO_2 nanocomposite for degradation of dye pollutants (methylene blue, texbrite BAC-L, texbrite BBU-L and texbrite NFW-L) under ultrasonic irradiation. Dye Pigment. 2016;134:487–97.
80. Atchudan R, Edison TNJI, Perumal S, Vinodh R, Lee YR. In-situ green synthesis of nitrogen-doped carbon dots for bioimaging and TiO_2 nanoparticles@ nitrogen-doped carbon composite for photocatalytic degradation of organic pollutants. J Alloys Compd. 2018;766:12–24.
81. Zhao D, Sheng G, Chen C, Wang X. Enhanced photocatalytic degradation of methylene blue under visible irradiation on graphene@TiO2 dyade structure. Appl Catal B Environ. 2012;111:303–8.
82. Wu F, Li X, Liu W, Zhang S. Highly enhanced photocatalytic degradation of methylene blue over the indirect all-solid-state Z-scheme g-C3N4-RGO-TiO_2 nano-heterojunctions. Appl Surf Sci. 2017;405:60–70.
83. Chen J, Shu J, Anqi Z, Juyuan H, Yan Z, Chen J. Synthesis of carbon quantum dots/TiO_2 nanocomposite for photo-degradation of Rhodamine B and cefradine. Diamond Relat Mater. 2016;70:137–44.
84. Hasan MT, Gonzalez-Rodriguez R, Ryan C, Faerber N, Coffer JL, Naumov AV. Photo- and electroluminescence from nitrogen-doped and nitrogen–sulfur codoped graphene quantum dots. Adv Funct Mater. 2018;28:1804337.
85. Jiqian Y, Xianlong Z, Dihua W, Xudong Z, Zhen Z. S-doped N-rich carbon nanosheets with expanded interlayer distance as anode materials for sodium-ion batteries. Adv Mater. 2017;29:1604108.
86. Munusamy S, Mandlimath TR, Swetha P, Al-Sehemi AG, Pannipara M, Koppala S, Shanmugam P, Boonyuen S, Pothu R, Boddula R. Nitrogen-doped carbon dots: Recent developments in its fluorescent sensor applications. Environ Res. 2023;231(Pt 1):116046. https://doi.org/10.1016/j.envres.2023.116046.
87. Xu Q, Kuang T, Liu Y, Cai L, Peng X, Sreenivasan Sreeprasad T, Zhao P, Yu Z, Li N. Heteroatom-doped carbon dots: synthesis, characterization, properties, photoluminescence mechanism and biological applications. J Mater Chem B. 2016;4(45):7204–19. https://doi.org/10.1039/c6tb02131j.
88. Miao S, Liang K, Zhu J, Yang B, Zhao D, Kong B. Hetero-atom-doped carbon dots: Doping strategies, properties and applications. Nano Today. 2020;33:100879. https://doi.org/10.1016/j.nantod.2020.100879.
89. Sheikh MA, Chandok RS, Abida K. High energy density storage, antifungal activity and enhanced bioimaging by green self-doped heteroatom carbon dots. Discover Nano. 2023;18:132. https://doi.org/10.1186/s11671-023-03910-9.
90. Singh A, et al. Property modulation of graphene oxide incorporated with TiO_2 for dye-sensitized solar cells. ACS Omega. 2022;7(48):44170–9. https://doi.org/10.1021/acsomega.2c05637.
91. jahantigh F, Ghorashi SMB, Bayat A,. Hybrid dye sensitized solar cell based on single layer graphene quantum dots. Dyes Pigm. 2020. https://doi.org/10.1016/j.dyepig.2019.108118.
92. Padmanathan S, Prakasam A. Design and fabrication of hybrid carbon dots/titanium dioxide (CDs/TiO_2) photoelectrodes for highly efficient dye-sensitized solar cells. J Mater Sci Mater Electron. 2020;31:3492–9. https://doi.org/10.1007/s10854-020-02897-8.
93. Samir M, Agour AM, Ismail Z, Nageh H, Abdellatif SO. The impact of N-doped carbon quantum dots on dye-sensitized solar cells operating under diffused- and low-light intensity. IEEE J Photovolt. 2024. https://doi.org/10.1109/JPHOTOV.2023.3336474.
94. Yang Y, Zhu L, Sun H, Huang X, Luo Y, Li D, Meng Q. Composite counter electrode based on nanoparticulate PbS and carbon black: towards quantum dot-sensitized solar cells with both high efficiency and stability. ACS Appl Mater Interfaces. 2012;4(11):6162–8. https://doi.org/10.1021/am301787q.
95. Miao X, Pan K, Pan Q, Zhou W, Wang L, Liao Y, Tian G, Wang G. Highly crystalline graphene/carbon black composite counter electrodes with controllable content: synthesis, characterization and application in dye-sensitized solar cells. Electrochim Acta. 2013;96:155–63. https://doi.org/10.1016/j.electacta.2013.02.092.
96. Wu C-S, Chang T-W, Teng H, Lee Y-L. High performance carbon black counter electrodes for dye-sensitized solar cells. Energy. 2016;115:513–8. https://doi.org/10.1016/j.energy.2016.09.052.
97. Feng H, Zhang Y, Cui F. Enhanced photocatalytic activity of Cu_2O for visible light-driven dye degradation by carbon quantum dots. Environ Sci Pollut Res. 2022. https://doi.org/10.1007/s11356-021-16337-5.
98. Safardoust-Hojaghan H, SalavatiNiasari M. Degradation of methylene blue as a pollutant with N-doped graphene quantum dot/titanium dioxide nanocomposite. J Clean Prod. 2017;148:31–6.
99. Atchudan R, Edison TNJI, Perumal S, Vinodh R, Lee YR. In-situ green synthesis of nitrogen-doped carbon dots for bioimaging and TiO_2 nanoparticles@nitrogen-doped carbon composite for photocatalytic degradation of organic pollutants. J Alloys Compd. 2018;766:12–24.
100. Bi I, Williams I, Fodjo E, Amadou K, Albert T, Kong C. Enhancing the photocatalytic activity of TiO2 nanoparticles using green Carbon quantum dots. Int J Nano Dimens. 2022;13:144–54. https://doi.org/10.22034/IJND.2022.685460.
101. Hu X, Han W, Zhang M, et al. Enhanced adsorption and visible-light photocatalysis on TiO_2 with in situ formed carbon quantum dots. Environ Sci Pollut Res. 2022;29:56379–92. https://doi.org/10.1007/s11356-022-19810-x.
102. Sathish Kumar M, et al. TiO_2-carbon quantum dots (CQD) nanohybrid: enhanced photocatalytic activity. Mater Res Express. 2018;5:075502. https://doi.org/10.1088/2053-1591/aacbb9.
103. Tong S, Zhou J, Ding L, Zhou C, Liu Y, Li S, Meng J, Zhu S, Chatterjee S, Liang F. Preparation of carbon quantum dots/TiO_2 composites and application for enhanced photodegradation of rhodamine B. Colloids Surf A Physicochem Eng Asp. 2022;648:129342. https://doi.org/10.1016/j.colsurfa.2022.129342.
104. Duran F, Diaz-Uribe C, Vallejo W, Muñoz-Acevedo A, Schott E, Zarate X. Adsorption and photocatalytic degradation of methylene blue on TiO_2 thin films impregnated with Anderson-Evans Al-polyoxometalates: experimental and DFT study. ACS Omega. 2023;8(30):27284–92. https://doi.org/10.1021/acsomega.3c02657.

Publisher's Note Springer Nature remains neutral with regard to jurisdictional claims in published maps and institutional affiliations.